Calculations of dielectric properties from the superparaelectric model of relaxors

1993 J. Phys.: Condens. Matter 5 8773

(http://iopscience.iop.org/0953-8984/5/46/015)

J. Phys.: Condens. Matter 5 (1993) 8773–8792. Printed in the UK

Calculations of dielectric properties from the super-paraelectric model of relaxors

A J Bell

Laboratoire de Céramique, Ecole Polytechnique Fédérale Lausanne, CH 1015 Lausanne, Switzerland

Received 16 August 1993

Abstract. An ideal superparaelectric is treated as an ensemble of independent, coherently polarizing regions, of linear dimension λ, each of which behaves as a 'Devonshire ferroelectric', with transition temperature T_0, and local polarization, $P_s \sim (T - T_0)^{1/2}$. For sufficiently small λ, the direction of the local polarization vector can fluctuate with thermal energies, giving rise to a static permittivity, ϵ_s, which follows a modified Curie law: $\epsilon_s \sim (T - T_0)\lambda^3/T$. In addition, the peak in permittivity at T_0 is suppressed due to spatially uniform thermal fluctuations in the magnitude of the local polarization. The activation energy for the directional fluctuations increases with decreasing temperature: $E_a \sim (T - T_0)^2\lambda^3$, giving rise to Debye-type relaxation and peaks in the real and imaginary permittivity around T_m, where $T_0 - T_m$ increases with decreasing λ. For a fictitious superparaelectric, based on $Pb(Zr_{0.7}Ti_{0.3})O_3$, the effects described above become important for $\lambda \leqslant 15$ nm. Relaxor-like frequency dependence of the imaginary part of the permittivity, ϵ'', is only observed when distributions of λ, width $\Delta\lambda$, are introduced. The best qualitative match to typical relaxor behaviour is seen when both λ and $\Delta\lambda$ diverge at some non-zero temperature. The introduction of dipolar coupling, in the form of a mean field, produces a transition to a macroscopic ferroelectric state in the static properties, at a temperature which increases with increasing coupling strength. For sufficiently strong coupling, a spontaneous transition may be apparent in observable time scales; otherwise the system remains glassy.

1. Introduction

The class of dielectrics known as 'relaxors' [1] are of significant technological and scientific interest. The class comprises a large number of complex perovskites of the types $A(B'_xB''_{1-x})O_3$, (e.g. $Pb(Mg_{1/3}Nb_{2/3})O_3$ (PMN), $Pb(Sc_{1/2}Ta_{1/2})O_3$ (PST) and $Pb(Sc_{1/2}Nb_{1/2})O_3$ (PSN)), some perovskite solid solutions (e.g. $(Pb_{1-3x/2}La_x)(Zr_{1-y}Ti_y)O_3$ (PLZT) and $(Pb_{1-x}Ba_x)(Zr_{1-y}Ti_y)O_3$ (PBZT)) and a number of tungsten bronze structure oxides (e.g. $Sr_{5-x}Ba_xNb_{10}O_{30}$ (SBN)). They are characterized by a broad peak in the real part of the dielectric permittivity as a function of temperature, with the peak decreasing in magnitude and shifting to higher temperature with increasing measurement frequency in the RF range (figure 1(a)). At temperatures below that of the peak permittivity, the real part decreases in magnitude with increasing frequency. The imaginary part of the dielectric permittivity exhibits frequency dependence at temperatures above its peak value, with the peak value increasing with increasing frequency (figure 1(b)).

In PMN the temperature of the maximum permittivity is around 270 K. At temperatures above 600 K, the real part of permittivity follows Curie–Weiss behaviour [2], with a Curie temperature of 398 K. This is consistent with the observations of Burns [3], who showed that local polarization fluctuations exist up to 600 K.

0953-8984/93/468773+20$07.50

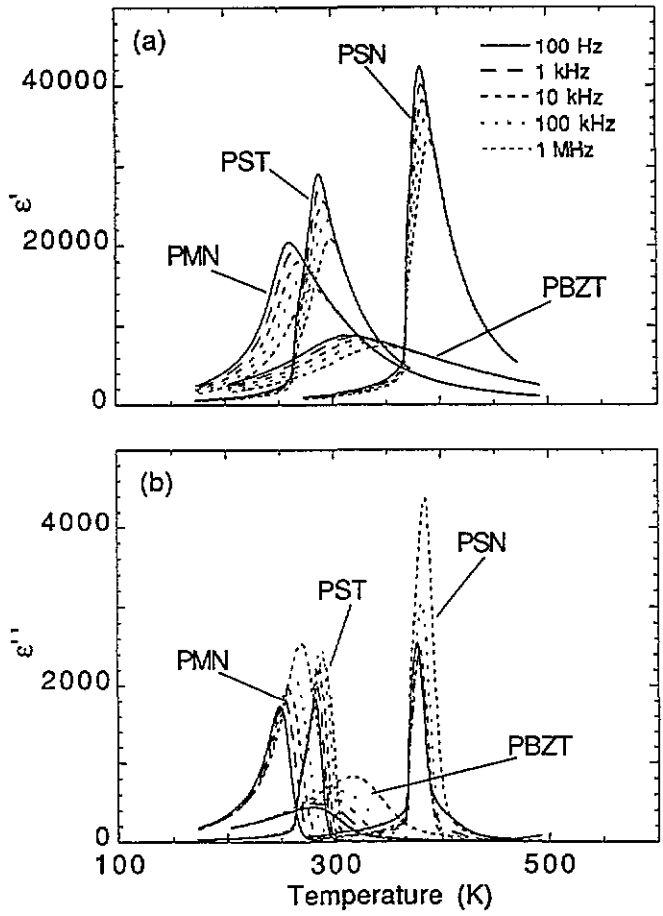

Figure 1. (*a*) Real and (*b*) imaginary parts of permittivity of PMN, PST, PSN and PBZT as a function of temperature.

Relaxor behaviour is associated with a gradual transition from macroscopic paraelectric to a ferroelectric phase at a temperature below that of the peak in permittivity. In PMN and PLZT the ferroelectric phase is induced by the application of an electric field, the transition temperature being dependent upon the applied field strength [4]. In PMN zero-field depoling occurs on heating at 213 K. In contrast, in PST and PSN, spontaneous, zero-field transitions to a ferroelectric state, the appearance of which has been shown to be critically dependent upon the Pb-vacancy concentration, occur at 263 K and 368 K respectively, with the dielectric maxima at approximately 28K and 383 K respectively [5].

It has been recognized since the earliest investigations of relaxor behaviour [6] that crystalline disorder plays an important role in the phenomenon. Setter and Cross [7] showed that PST with high degrees of B-site ordering is ferroelectric, whilst that with disorder on the B site is a relaxor. Transmission electron microscopy of PMN [8,9] has revealed a partitioning of the structure into ordered and disordered regions at the nanometre scale. Whilst x-ray and neutron diffraction studies [10] have shown that high-temperature PMN is macroscopically cubic, but with significant atomic shifts around the ideal perovskite

structure. On cooling, correlated polar clusters with ⟨111⟩ distortions develop leading to the formation, at low temperature, of polar nanodomains with an estimated diameter of 10 nm at 5 K.

It has been suggested that the dielectric anomaly and frequency dispersion are due to the slowing down of superparaelectric moments [1]. An ideal superparaelectric might be considered to be an ensemble of small polar regions, the sizes of which are characterized by the spatial coherence of their spontaneous polarization. (There is a multiplicity of terms in the relaxor literature for such basic entities. They have been referred to in various experimental and theoretical contexts as micro-domains, nano-domains, clusters and Känzig regions. In the present work, the term cluster will be used to represent a small coherently polarizing volume. This does not necessarily imply correspondence with the term as used in the orientational glass literature [11], for example.) Where the size of the clusters is sufficiently small, such that the energy required to reorient the polarization is of the order of the thermal energy of the crystal, the direction of the polarization of each cluster can fluctuate. On reducing the temperature of the crystal, the frequency of the fluctuations will decrease. Such a situation would be expected to give rise to a classical Debye-like relaxation in the dielectric properties, with a temperature-dependent relation frequency. The observed transition in PST might correspond to a spontaneous alignment of superparaelectric clusters to form a macroscopic ferroelectric state. On the other hand the moments in PMN appear to slow down into a glassy state.

Previous analysis of the dielectric behaviour suggests that the slowing down of the clusters is more rapid than simple Debye behaviour would predict [12]. Subsequently, the frequency dispersion of PMN has been analysed according to Vogel–Fulcher relationship:

$$f_m = f_v \exp(-E_v/k(T_m - T_f))$$

in which T_m is the temperature of the peak in permittivity for measurement frequency f_v; T_f is known as the freezing temperature. Values of E_v equivalent to 464 K and $f_v = 10^{12}$ Hz were obtained [13]. T_f was found to be 218 K, almost coincident with the zero-field depoling temperature. It has been argued that similar behaviour in PLZT, and by implication in PMN, is indicative of freezing of the superparaelectric moments into a dipolar glassy state due to correlations between moments [4]. Essentially this is in agreement with the recent conclusions from acoustic data [14], that the low-temperature state of PMN corresponds to a dipolar glass state with ferroelectric order. Other possibilities discussed in the literature include a dipolar glass without ferroelectric order [14] and ferroelectric nano-domains stabilized by random fields due to compositional fluctuations [15].

Much emphasis has been placed upon the broadening of the relaxation time spectrum of relaxors with decreasing temperature, as inferred from measurements of the dielectric function [14, 16]. Recently Tagantsev [17] has shown that the Vogel–Fulcher relationship can be a direct consequence of a gradual broadening of a relaxation time spectrum and that the relationship is not necessarily indicative of a system in which the spectrum becomes infinitely broad at T_f, but implies only gradual broadening. The majority of measurements of relaxors cover a comparatively small range of frequencies, typically 10 Hz to 1 MHz. Over such a range, a broad, but not necessarily infinitely broad, spectrum of relaxation times would appear to exhibit frequency independence in the imaginary part of permittivity. Only by looking over a wider range of frequencies may some frequency dependence be detected. Recently, Colla *et al* [18], from measurements of PMN down to 10^{-3} Hz, inferred a broad, but finite, frequency spectrum, of which the mean was approximately linearly temperature dependent down to 230 K, but then appeared constant ($\approx 10^{-5}$ Hz) at lower temperatures.

It is the purpose of the present work to provide a foundation upon which numerical calculations of the dielectric behaviour of an ensemble of superparaelectric clusters may be carried out and with which different models of cluster dynamics may be examined. A basic assumption of the calculations is that initially the clusters may be treated as independent, classical ferroelectrics. The main justification for this assumption is that at high-temperature Curie–Weiss behaviour is apparent. The approach taken is phenomenological rather than microscopic and employs the Landau–Ginzberg–Devonshire (LGD) formalism for ferroelectrics to calculate the dielectric function of an ensemble of clusters. Although the LGD theory is often regarded as inaccurate far from the Curie temperature, its application to the PZT system [19–23] over a wide temperature range has been shown to be successful. For the illustrative calculations here, it provides a convenient approximation for the basis of the model. The Debye model of dielectric relaxation is assumed to apply to the ensemble. As examples of how the dielectric behaviour of different scenarios may be compared, calculations are performed for a number of fictional superparaelectrics based upon $Pb(Zr_{0.7}Ti_{0.3})O_3$: initially, an ensemble of independent, identical, mono-sized superparaelectric clusters, and subsequently, (i) a distribution in the size of the clusters, (ii) temperature-dependent cluster sizes, and (iii) dipolar cluster interactions.

2. Theoretical analysis

2.1. Debye relaxation of an ideal superparaelectric

For the purpose of these calculations, an ideal superparaelectric is defined as an ensemble of non-interacting polar regions, in which each region, or cluster, behaves as an independent, conventional ferroelectric. The size of the polar regions is such that the direction of polarization may be reoriented by thermal fluctuations of the lattice. This is perhaps consistent with the concept of a ferroelectric crystal which includes features, such as crystalline disorder, which limit the coherence of the spontaneous polarization. The density of these features determines the size of a coherently polarizing volume, λ. In the simplest case, each initially isotropic region is subject to distortion, on cooling through temperature T_0, to a ferroelectric structure characterized by a local, temperature-dependent polarization, P_s. The reorientation of the polarization vector of a single region, between the variants allowed by the crystal symmetry, is considered to be a thermally activated process with activation energy E_a. In terms of an energy density, G_a, the activation energy is dependent on the region size ($E_a = G_a\lambda^3$) and is assumed to be a function of the local polarization P_s. For E_a of the order of kT, the polarization vector fluctuates in direction with frequency, f_r, given by:

$$f_r = f_0 \exp\left(\frac{-G_a\lambda^3}{kT}\right) \tag{1}$$

in which f_0 is a frequency of the order of the crystal phonon frequencies. In the case of a second order ferroelectric phase transition, the value of P_s is proportional to $(T_0 - T)^{1/2}$; G_a therefore increases and f_r decreases with decreasing temperature below T_0. A temperature-dependent dielectric relaxation is therefore observed at frequencies below f_0, with the dielectric function being given by the Debye equations:

$$\epsilon' = \epsilon_\infty + \frac{\epsilon_s - \epsilon_\infty}{1 + (f/f_r)^2} \qquad \epsilon'' = \frac{(\epsilon_s - \epsilon_\infty)(f/f_r)}{1 + (f/f_r)^2} \tag{2}$$

in which ϵ_s is the static permittivity and ϵ_∞ the permittivity for $f \gg f_r$. Both the static and high-frequency permittivities might be expected to be temperature dependent. ϵ_∞ represents changes in the magnitude of the polarization vector under applied fields at frequencies higher than the relaxation frequency and includes both ionic and electronic contributions; it is that permittivity which would be exhibited by a corresponding 'macroscopic' ferroelectric at frequencies $\leqslant f_0$, i.e. not the optical permittivity. The static permittivity, ϵ_s represents the change in polarization due to reorientation of the polarization vector under static applied fields.

For the purpose of illustration the example followed here considers the case of a superparaelectric perovskite with low-temperature rhombohedral symmetry. To simplify the analysis, the ferroelectric transition will be assumed to be second order.

2.2. *Static permittivity*

A rhombohedral ferroelectric of the perovskite structure possesses eight possible equivalent directions for the polarization vector. On the application of a field, E, parallel to one of these directions the energy of each of the directions is modified by the appropriate component of $-EP_s\lambda^3$. That is, the energy state of regions with polarization parallel to the direction of the applied field will be modified by $-EP_s\lambda^3$, the anti-parallel direction by $EP_s\lambda^3$, three directions by $EP_s\cos(\alpha)\lambda^3$ and three directions by $-EP_s\cos(\alpha)\lambda^3$, where α is the angle between the $\langle 111 \rangle$ directions. The total static polarization parallel to the applied field, due to cluster reorientation, is therefore given by:

$$\begin{aligned} P_t = P_s\Big[&\exp(EP_s\lambda^3/kT) - \exp(-EP_s\lambda^3/kT) + 3\cos(\alpha)\exp(EP_s\cos(\alpha)\lambda^3/kT) \\ &- 3\cos(\alpha)\exp(-EP_s\cos(\alpha)\lambda^3/kT)\Big] \\ &\times \Big[\exp(EP_s\lambda^3/kT) \\ &+ \exp(-EP_s\lambda^3/kT) + 3\exp(EP_s\cos(\alpha)\lambda^3/kT) \\ &+ 3\exp(-EP_s\cos(\alpha)\lambda^3/kT)\Big]^{-1}. \end{aligned} \tag{3}$$

When the rhombohedral distortion is small compared to the cubic prototype,

$$\cos(\alpha) \approx 1/3$$

and

$$P_t = P_s \tanh\left(\frac{EP_s\lambda^3}{3kT}\right). \tag{4}$$

The static permittivity is given by differentiating P_t with respect to the field, which for the limit $E \to 0$, reduces to the Curie law. Including contributions from the change in magnitude of the polarization vector, that is the high-frequency permittivity, ϵ_∞, the static permittivity, for $T < T_0$, is given as:

$$\epsilon_s = \frac{P_s^2\lambda^3}{3kT} + \epsilon_\infty. \tag{5}$$

2.3. Local polarization

The polarization, high-frequency permittivity and anisotropy energy density may all be found in terms of the LGD theory of ferroelectrics [24]. The elastic Gibbs free energy of a ferroelectric, with reference to the unpolarized state, is expressed in terms of a Taylor series expansion in polarization. For simplicity, the series is terminated here in terms of P^4, which is sufficient for second-order transitions, but not necessarily accurate.

$$G_1 - G_{10} = \alpha_1\left(P_1^2 + P_2^2 + P_3^2\right) + \alpha_{11}\left(P_1^4 + P_2^4 + P_3^4\right) + \alpha_{12}\left(P_1^2P_2^2 + P_2^2P_3^2 + P_3^2P_1^2\right) \tag{6}$$

where $P_{i=1,2,3}$ are the components of polarization parallel to the pseudo-cubic axes and α_1 is temperature dependent:

$$\alpha_1 = \alpha_1'(T - T_0). \tag{7}$$

For rhombohedral symmetry

$$P_1 = P_2 = P_3 = P_r.$$

Therefore the expression reduces to

$$\Delta G_1 = G_1 - G_{10} = 3\alpha_1 P_r^2 + 3(\alpha_{11} + \alpha_{12})P_r^4. \tag{8}$$

The stable states are found by solving

$$\mathrm{d}\Delta G_1/\mathrm{d}P_r = 0$$

to give the well known result for the temperature dependence of the polarization:

$$P_r^2 = \frac{-\alpha_1'(T - T_0)}{2(\alpha_{11} + \alpha_{12})} \qquad (T < T_0) \tag{9}$$

with

$$P_s^2 = 3P_r^2.$$

For macroscopic crystals, the stable state polarization is taken to be that corresponding to the minimum in ΔG_1. However, for an ensemble of clusters, if the size is such that $\Delta G_1\lambda^3$ is of the order of kT, a distribution of states about the minimum energy should be considered. This would imply a corresponding distribution in the magnitude of polarization and permittivity, ϵ_∞. The distribution is most significant when the potential well is shallow,

that is, close to T_0. Such a situation has been considered recently for the dielectric properties of 'sub-grains' in $BaTiO_3$ ceramics [25]. For complete rigour the mean local polarization should be calculated by integrating over the three components of polarization $P_{i=1,2,3}$, however the result is similar if it is assumed, for the sake of computational brevity, that only distributions of the local polarization parallel to the applied field are significant. Hence, averaging of the polarization is accomplished by integrating over possible values in the ⟨111⟩ direction only:

$$\bar{P}_s = \int_0^\infty P_s \exp\left(-G_1(P_s)\lambda^3/kT\right) dP_s \Big/ \int_0^\infty \exp\left(-G_1(P_s)\lambda^3/kT\right) dP_s \tag{10}$$

where $G_1(P_s)$ is given by equation (6) with $P_s^2 = 3P_r^2$ ($P_1 = P_2 = P_3$), and $G_{10} = 0$. For $T > T_0$, the free energy surface is isotropic, thus the ⟨111⟩ direction is representative of the isotropic polarization fluctuations. In this region, equation (10) has an analytical solution of the form:

$$\bar{P}_s = \frac{\sqrt{3\alpha_1}U_{1,3/2}(2\Gamma)}{2\sqrt{\alpha_{11}+\alpha_{12}}e^{\Gamma}K_{1/4}(\Gamma)} \tag{11}$$

where

$$\Gamma = 3\alpha_1^2\lambda^3][8(\alpha_{11}+\alpha_{12})kT]$$

and where $U_{x,y}(\,)$ is the confluent hypergeometric function and $K_z(\,)$ the modified Bessel function. However, this solution is only valid for $\alpha_1 > 0$; numerical solutions must be sought for $T < T_0$.

2.4. High-frequency permittivity

Following normal practice for macroscopic ferroelectrics, the value of ϵ_∞ is found from the second differential of the free energy with respect to polarization. In terms of the dielectric stiffness

$$\eta_{ij} = \partial^2 \Delta G_1 / \partial P_i \partial P_j$$

the stiffness perpendicular and parallel to the polar axis are then given by:

$$\eta'_{11} = \eta'_{22} = \eta_{11} - \eta_{12} = -2\alpha_1 \frac{2\alpha_{11} - \alpha_{12}}{\alpha_{11} + \alpha_{12}}$$

and

$$\eta'_{33} = \eta_{11} + 2\eta_{12} = -4\alpha_1. \tag{12}$$

For $T > T_0$

$$\eta_{11} = \eta_{22} = \eta_{33} = 2\alpha_1. \tag{13}$$

Using these relations, the stiffness, and hence the high-frequency permittivity of an ensemble of randomly oriented clusters, parallel to a ⟨111⟩ axis of the crystal can be estimated. However, as with the calculation of polarization, it is necessary to take into account the effect of thermal fluctuations on the magnitude of polarization, necessitating an averaging of the stiffness over probable values:

$$\bar{\eta} = \int \eta(P_s) \exp\left(-G_1(P_s)\lambda^3/kT\right) \mathrm{d}P_s \Big/ \int \exp\left(-G_1(P_s)\lambda^3/kT\right) \mathrm{d}P_s. \tag{14}$$

No analytical solution has been found for $T < T_0$ necessitating numerical integration, but for $T > T_0$:

$$\bar{\eta} = 2\alpha_1 + \frac{3\alpha_1}{2} \frac{\sqrt{\pi} U_{5/4,3/2}(2\Gamma)}{(2\Gamma)^{1/4} e^{\Gamma} K_{1/4}(\Gamma)} \tag{15}$$

2.5. Anisotropy energy density

G_a can be calculated from the free energy expansion as being the lowest-energy path for reorientation of the polarization between two ⟨111⟩ directions. Figure 2 shows the free energy surface for $T < T_0$ calculated for $Pb(Zr_{0.7}Ti_{0.3})O_3$ from the free energy coefficients given by Haun [19–23]. The x axis represents the value of P_1 whereas the y axis shows the value of P_2. The value of P_3 is constrained to be equal to P_2 such that the minima corresponding to the four stable symmetries of the system (cubic, tetragonal, rhombohedral and orthorhombic) can be shown on one diagram. The absolute minima in free energy of the system can be seen to lie on the lines $P_1 = P_2$ $(= P_3)$, whereas secondary minima exist for values of $P_1 = 0$ (orthorhombic) and P_2 $(= P_3) = 0$ (tetragonal). These correspond to the ⟨111⟩, ⟨011⟩ and ⟨001⟩ directions of the polarization vector respectively. The activation energy for orientation from one rhombohedral orientation to another is the difference between the energy of the rhombohedral state and that corresponding to the orthorhombic orientation of polarization (⟨011⟩ direction). From (6) and (9) above, the energy of the rhombohedral and orthorhombic states are given by:

$$G_r = -\frac{3}{4} \frac{\alpha_1^2}{4\alpha_{11} + \alpha_{12}}$$

and

$$G_0 = -\frac{\alpha_1^2}{2\alpha_{11} + \alpha_{12}} \tag{16}$$

and $G_a = G_0 - G_r$:

$$G_a = \alpha_1^2 \frac{2\alpha_{11} - \alpha_{12}}{4(\alpha_{11} + \alpha_{12})(2\alpha_{11} + \alpha_{12})}. \tag{17}$$

Thus, the activation energy for reorientation of the polarization is proportional to $(T - T_0)^2$, and hence, the Debye relaxation frequency does not follow true Arrhenius-type behaviour. Fluctuations in the magnitude of polarization might be expected to produce a distribution of activation energies. Whilst, for certain temperature ranges, this distribution is assumed to have some importance, its effect is likely to be similar to that of having a distribution of cluster sizes, (a case which is examined in some detail below), therefore in the simple case examined initially, the effects on G_a of fluctuations in the magnitude of polarization are omitted.

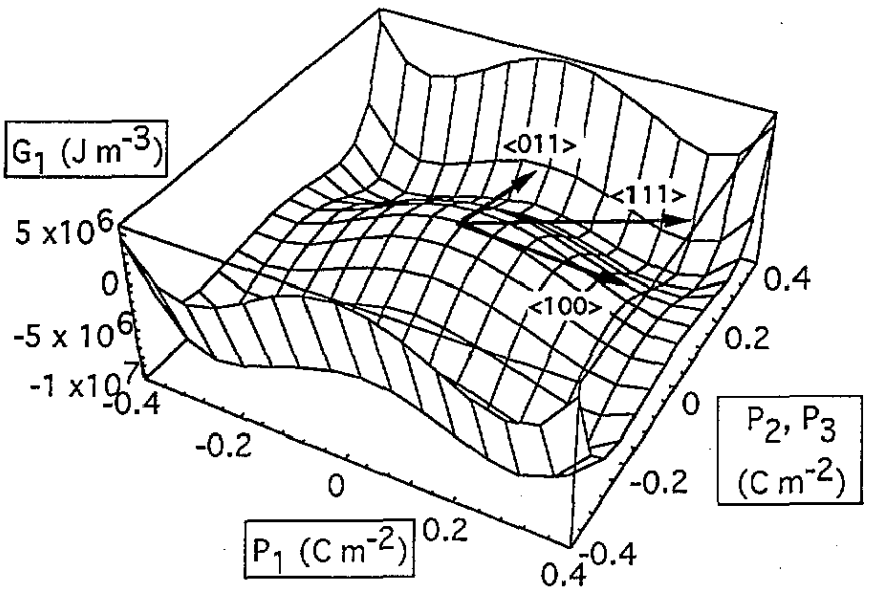

Figure 2. Free energy surface of a ferroelectric perovskite with rhombohedral symmetry for $T < T_0$. Calculated for $Pb(Zr_{0.7}Ti_{0.3})O_3$.

3. Results

3.1. Independent mono-sized clusters

All the terms in the Debye equations (2) are functions of the six variables: α_1', α_{11}, α_{12}, T_0, λ and f_0. For an increasing number of macroscopic ferroelectrics, the free energy coefficients are known, hence it is possible to calculate a fictional superparaelectric dielectric function

for such materials with only the region size λ, and the relaxation frequency pre-exponent, f_0, as parameters.

As an example, calculations are made here for $Pb(Zr_{0.7}Ti_{0.3})O_3$ (PZT 70/30), which is a perovskite with a second order transition from a paraelectric to a rhombohedral ferroelectric phase at 605 K. Although at present there is little evidence to suggest that PZT 70/30 is itself a relaxor, it is close to two known relaxor systems: $(Pb_{1-x}La_x)(Zr_{1-y}Ti_y)O_3$ and $(Pb_{1-x}Ba_x)(Zr_{1-y}Ti_y)O_3$. In the following simulations, terms in the free energy higher than P^4 are ignored, as are terms due to octahedral tilts or possible antiferroelectric ordering. The values of the free energy coefficients are those given by Haun [21]. The parameter f_0 is taken to be 10^{12} Hz, unless stated otherwise.

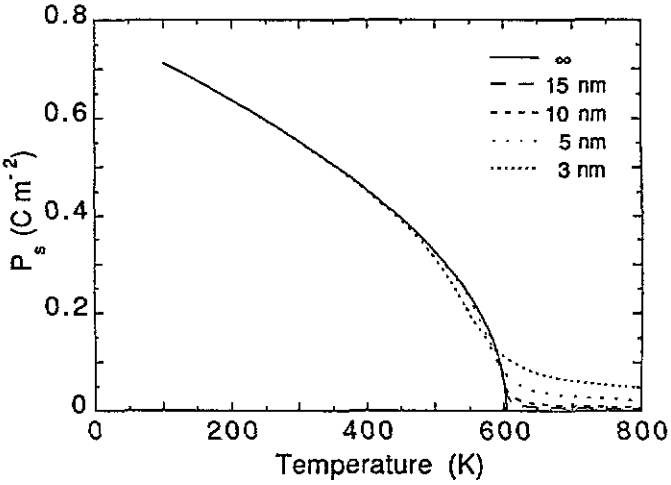

Figure 3. Mean local polarization of an ideal superparaelectric as a function of temperature for values of λ = 3 nm to ∞.

Figure 3 shows the mean local polarization, $\bar{P}_s$, as a function of temperature, including the effects of fluctuations in the magnitude of polarization (equation (10)), with the cluster size as a parameter. Below T_0, there are minor deviations from macroscopic behaviour for the smallest cluster sizes, however, the calculation shows that the mean local polarization is always non-zero for $T > T_0$. For the larger cluster sizes, $\bar{P}_s$ approaches zero asymptotically within 50 K above T_0, however, for smaller clusters the materials exhibit significant values of mean polarization towards the decomposition temperature of the material.

The corresponding mean high-frequency permittivity ($= (\bar{\eta}_0)^{-1}$) is shown in figure 4 as a function of temperature. The height of the peak in permittivity at T_0 decreases with decreasing cluster size and becomes rather insignificant for cluster diameters of < 10 nm. For temperatures $(T_0 - 100) > T > (T_0 + 200)$ the mean permittivity approximates to that for macroscopic sizes. The upper limit of this range is similar to that seen for PMN in its departure from Curie–Weiss behaviour [2], ($T_{\text{Burns}} \simeq T_0 + 200$).

The static permittivity, ϵ_s, is shown in figure 5 with the region size, λ, as a parameter. The corresponding real and imaginary parts of the relative permittivity at 1 kHz are shown in figure 6. The frequency dependence of the complex permittivity is shown for λ = 3 nm in figure 7.

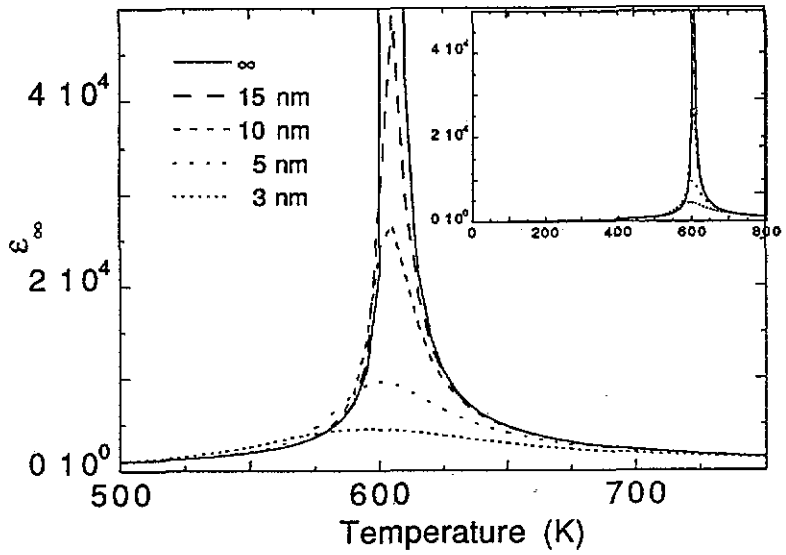

Figure 4. Mean high-frequency permittivity of an ideal superparaelectric as a function of temperature for values of λ = 3 nm to ∞. Results for the full temperature range are shown inset.

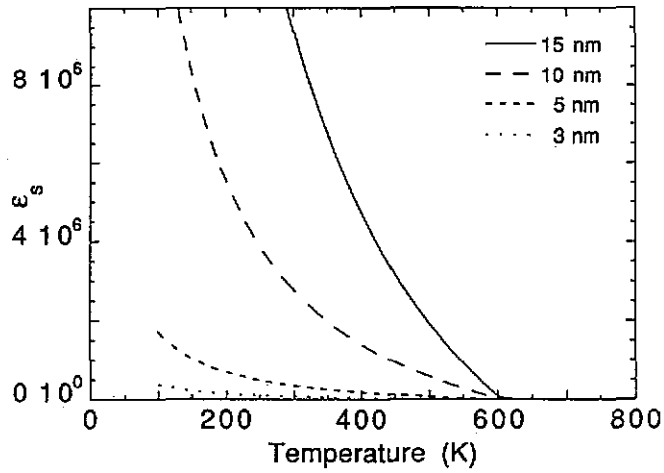

Figure 5. Static permittivity of an ideal superparaelectric as a function of temperature for values of λ = 3 nm to 15 nm.

It is clear that the $\exp((T - T_0)^2\lambda^3/T)$ dependence of the relaxation frequency is responsible for the marked peak and dispersion in the permittivities, the temperature of peak permittivity decreasing with decreasing cluster size. The peaks shown in figures 6 and 7 are due purely to the slowing down of the superparaelectric moments, with only a minor contribution from the paraelectric–superparaelectric transition at 605 K.

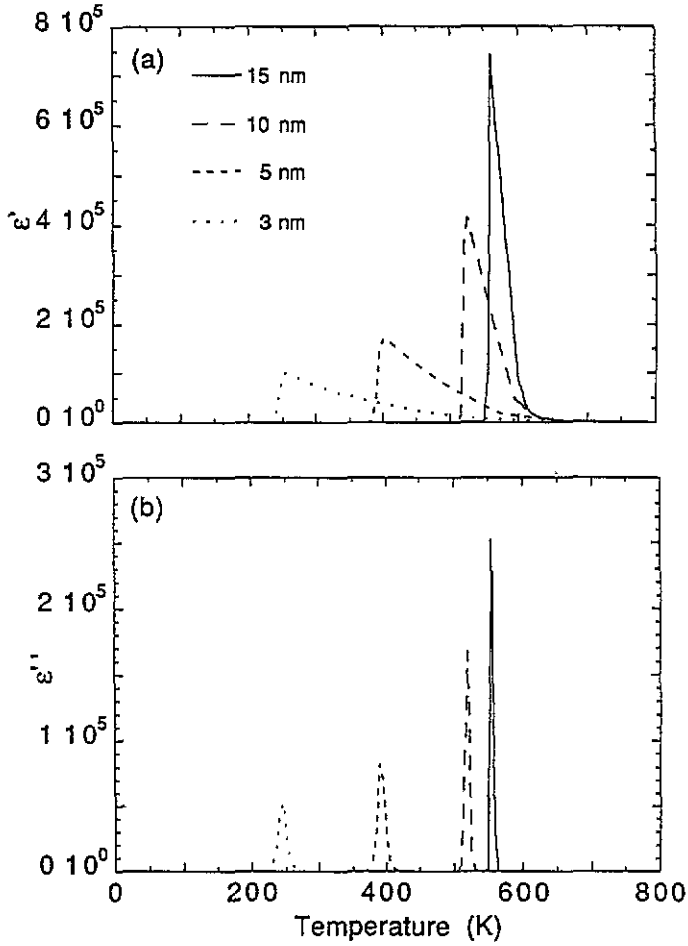

Figure 6. (*a*) Real and (*b*) imaginary parts of permittivity at 1 kHz as a function of temperature for values of $\lambda = 3$ nm to 15 nm.

3.2. Cluster size distributions

It is clear from the large values of permittivity predicted by the above model for large clusters and from the breadth of the permittivity peaks for the smaller clusters, that this calculated behaviour differs markedly from that exhibited by known relaxors. Moreover, the calculated imaginary part of the permittivity is contrary to that found experimentally; that is, the maximum ϵ'' increases as a function of frequency, with no tendency towards frequency independence at lower temperatures. These disparities can perhaps be attributed to the use of unique values of T_0 and λ in the calculations, both of which may be expected to be represented by a distribution of values in real systems. In the present model, due to the $\exp((T - T_0)^2\lambda^3/T)$ dependence of the relaxation frequency, any distribution in T_0 or λ, as might be expected in a disordered crystal, would result in a broadening in the relaxation time spectrum with decreasing temperature. Hence, it is relevant to look at least one of these cases in more detail.

It is not obvious how a distribution of contributions to the complex permittivity may be

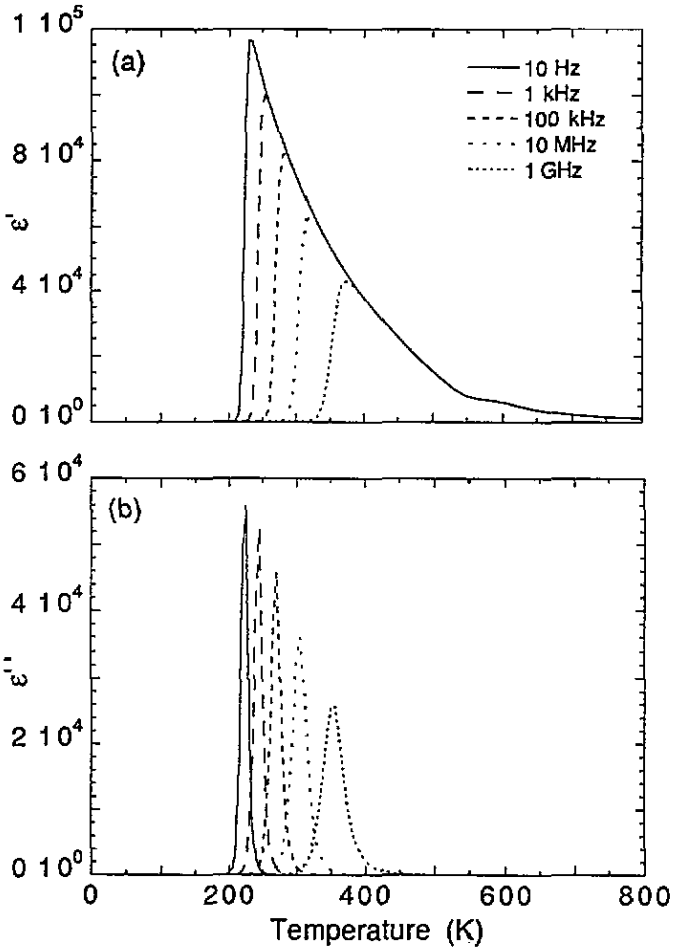

Figure 7. (*a*) Real and (*b*) imaginary parts of permittivity as a function of temperature and frequency for $\lambda = 3$ nm.

summed. Here the approach has been to sum the real and imaginary parts separately. As in any mixture of dielectrics, the problem may be approached from the point of summing the permittivity or the stiffness; in equation (14) the latter was used. Experience has shown that these two approaches represent limiting cases only, whilst various empirical approaches have been proposed which provide better fits to experiment [26]. Somewhat arbitrarily, the form chosen here is a summation over stiffness for the real part of permittivity, whilst a summation of permittivities is used for the imaginary part. In general, the temperature and frequency dependences of the mean real permittivity, resulting from the two types of summation, is similar, but with a difference of approximately a factor of four in the peak value, the summation over stiffnesses provides the lower value. Here, log Gaussian distributions of λ were incorporated into the calculations as follows:

$$\epsilon' = \left[\int_{\lambda_-}^{\lambda_+} \exp\left(\frac{-(\log(\bar{\lambda}/\lambda))^2}{(\Delta\log\lambda)^2}\right)\left(\epsilon_\infty + \frac{(\epsilon_s - \epsilon_\infty)}{1+(f/f_r)^2}\right)^{-1} d\lambda\right]^{-1} \times \int_{\lambda_-}^{\lambda_+} \exp\left(\frac{-(\log(\bar{\lambda}/\lambda))^2}{(\Delta\log\lambda)^2}\right) d\lambda$$

$$\epsilon'' = \int_{\lambda_-}^{\lambda_+} \exp\left(\frac{-(\log(\bar{\lambda}/\lambda))^2}{(\Delta\log\lambda)^2}\right)\left(\frac{(\epsilon_s - \epsilon_\infty)(f/f_r)}{1+(f/f_r)^2}\right) d\lambda \times \left[\int_{\lambda_-}^{\lambda_+} \exp\left(\frac{-(\log(\bar{\lambda}/\lambda))^2}{(\Delta\log\lambda)^2}\right) d\lambda\right]^{-1}. \quad (18)$$

To avoid prohibitively lengthy computations due to multiple integrals, approximations were made, such that $\epsilon_\infty(T,\lambda) = \epsilon_\infty(T,\bar{\lambda})$ and $P_s(T,\lambda) = P_s(T,\bar{\lambda})$ leaving ϵ_s and f_r as the λ-dependent variables.

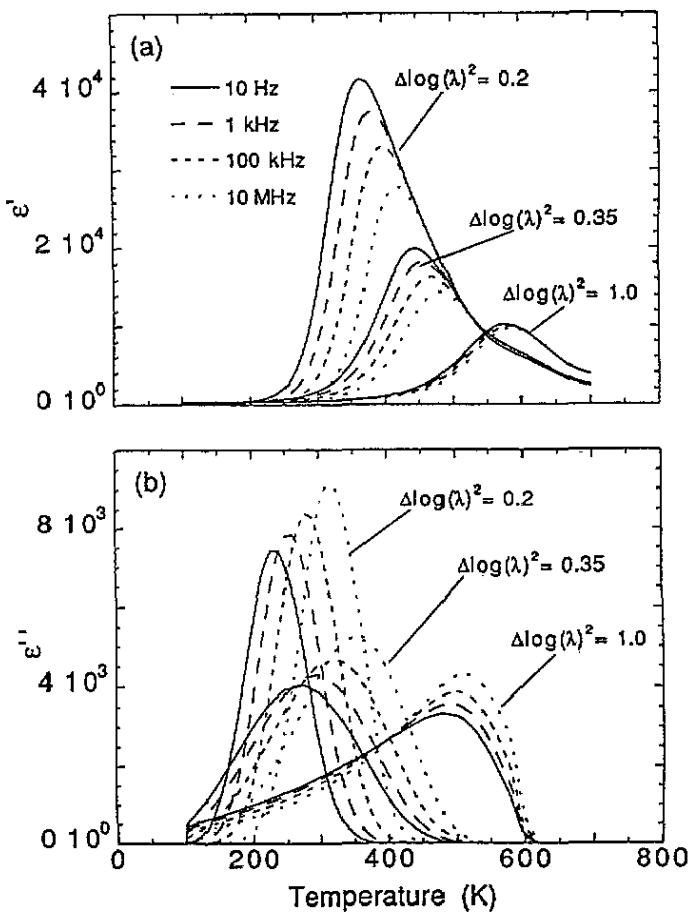

Figure 8. (*a*) Real and (*b*) imaginary parts of permittivity as a function of temperature and frequency for log Gaussian distributions of λ with $(\Delta\log\lambda)^2 = 0.2$, 0.35 and 1.0.

Figure 8 shows the real and imaginary parts of permittivity for $\bar{\lambda} = 3$ nm and distribution widths given by $(\Delta \log \lambda)^2 = 0.2$, 0.35 and 1. The lower limit of integration λ_- was chosen as 0.4 nm, the approximate dimension of the unit cell, whereas the upper limit, λ_+, was chosen as 100 nm. The imaginary part of permittivity shows evidence of the broadening of the relaxation time spectrum with decreasing temperature and increasing $\Delta \log \lambda$. However, with the parameters used here, the peak in ϵ'' for the largest value of $\Delta \log \lambda$ becomes extremely broad in the temperature domain when compared to experimental data (figure 1(*b*) for example). This perhaps suggests that the broadening of the relaxation frequency spectrum is stronger than that given by a temperature-independent distribution of cluster sizes, and that the cluster size distribution itself is temperature dependent.

3.3. Temperature-dependent cluster size

The suggestion that an increase in the size of the clusters takes place with decreasing temperature is supported not only from relaxation time data [14, 16], but also from estimates of the correlation radius of ferroelectric fluctuations estimated from neutron scattering data [27]. Examples have been calculated here by incorporating a simple size dependence into the above calculations (equation 20)), initially with $\bar{\lambda}(T) = \lambda_0/T$. For a log Gaussian distribution, the effect of increasing $\bar{\lambda}$ would bring about a corresponding increase in the linear width of the distribution, thus also fulfilling the requirement, suggested above, of a temperature-dependent distribution. An increase in cluster size with decreasing temperature gives narrower relaxation peaks at higher temperatures compared to the temperature-independent distributions. However, the requirement for maintaining a narrow peak in the temperature domain with a broad frequency spectrum suggests an even stronger temperature dependence of the size distribution. A number of simulations have been made which suggest that a divergence of both the cluster size and distribution width at a non-zero temperature might fulfill this condition. Figure 9 shows the real and imaginary parts of permittivity for log Gaussian distributions of λ, in which $\bar{\lambda} = \lambda_0(T - T_1)^{-1/2}$, where $T_1 = 400$ K and λ_0 is such that $\bar{\lambda}(T_0) = 3$ nm; f_0 is 10^{10} Hz. The form of the temperature dependence, reflecting the behaviour of the ferroelectric correlation length in Landau theory, was chosen as an illustration only and not as a physical hypothesis.

The peak in the real part of permittivity in figure 9 obeys the Vogel–Fulcher law, with the freezing temperature, $T_f = 484.3$ K, $f_v = 2.2 \times 10^{15}$ Hz and $E_v/k = 856.7$ K. The value of f_v is somewhat higher than that seen experimentally, however T_f and E_v are not dissimilar from what might be expected from an empirical familiarity of the Vogel–Fulcher behaviour of relaxors.

3.4. Dipolar interactions

The phenomenon of cluster coarsening might be considered as a departure from one of the basic assumptions of the ideal case, that is, the coupling between the clusters is negligible. Cluster growth can be interpreted as being equivalent to non-negligible interactions between clusters, which increase with decreasing temperature. It is therefore of some importance to examine even the most simple departure from the uncoupled case. The most elementary type of interaction might be considered is dipolar, as previously discussed by Viehland [16], and is developed here, in the form of a mean field, for the case of an ensemble of clusters of a single, temperature-independent size. It is assumed that the field experienced by a dipolar region due to the neighbouring dipoles is spatially uniform and proportional to the total polarization. In this way the expression for the static polarization due to applied fields

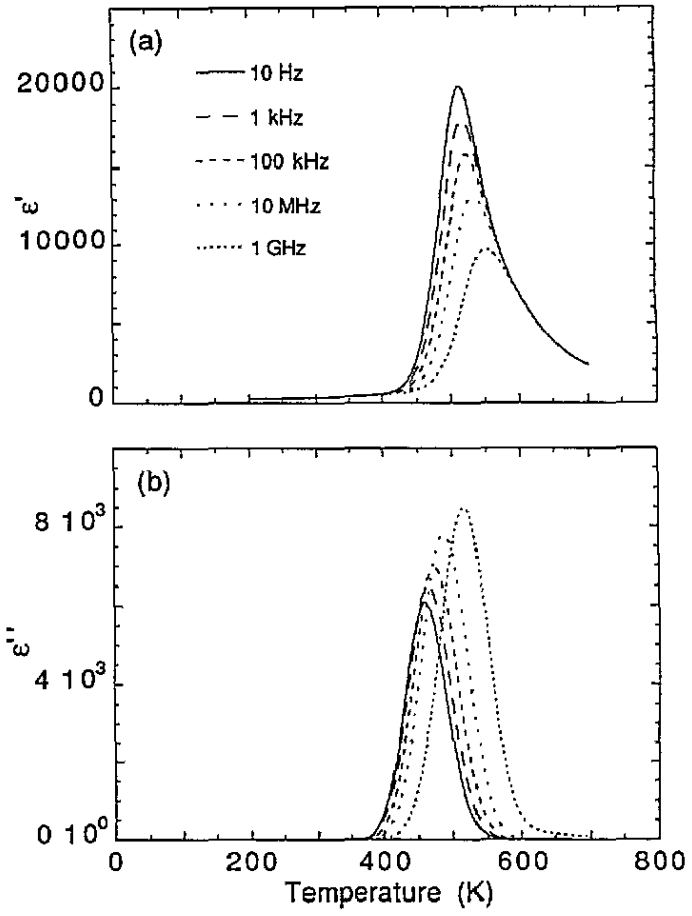

Figure 9. (*a*) Real and (*b*) imaginary parts of permittivity as a function of temperature for a log Gaussian distribution of cluster sizes with $(\Delta \log \lambda)^2 = 0.2$ and $\bar{\lambda}(T) = \lambda_0(T - T_1)^{-1/2}$ where $\bar{\lambda}(T_0) = 3$ nm, $T_1 = 400$ K and $f_0 = 10^{10}$ Hz.

(equation (3)) may be modified by additional energy terms within the exponentials, of the form $\gamma P_s P_t \lambda^3$. For $\cos(\alpha) = 1/3$, this gives:

$$P_t = P_s \tanh\left(\frac{(E + \gamma P_t) P_s \lambda^3)}{3kT}\right). \tag{19}$$

For the case where $E = 0$, this gives the static polarization at zero field. Figure 10 shows the calculated value of $P_t(E = 0)$ in comparison with P_s, the local polarization, for $\lambda = 3$ nm and $\gamma = 0.5 \times 10^6$ to 4.0×10^6 m F^{-1}. The corresponding behaviour of static permittivity, ϵ_s calculated for a small applied field ($E = 1000$ V m^{-1}) is shown in figure 11. With increasing γ, the temperature of the transition to a correlated polar state occurs at higher temperatures. When the temperature of the transition is in the region where the relaxation time is within observable limits one would expect to see a spontaneous transition

from a superparaelectric to a ferroelectric state, whereas for lower temperatures, when the relaxation time is much longer than observable experiments, the transition to the correlated state would only be observed after the application of some external stress, such as an electric field.

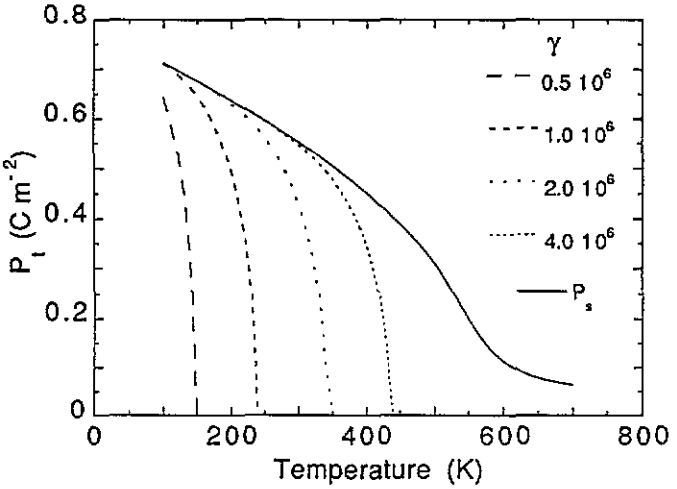

Figure 10. Static polarization as a function of temperature for mean-field dipolar interactions with $\gamma = 0.5 \times 10^6$ to 4.0×10^6 m F^{-1}. The local polarization, P_s, is shown for comparison.

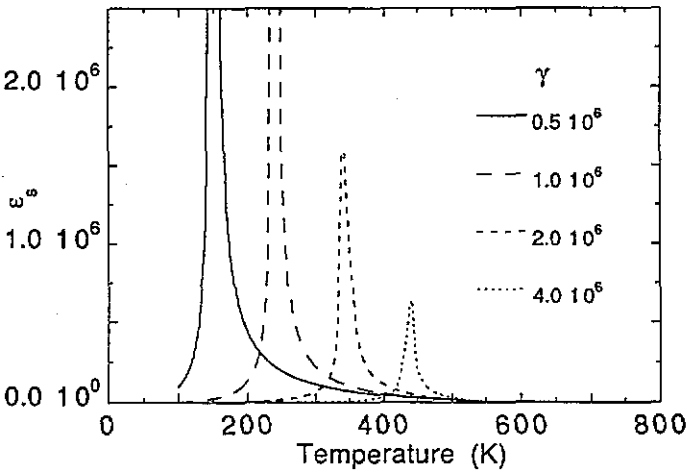

Figure 11. Static permittivity for mean-field dipolar interactions with $\gamma = 0.5 \times 10^6$ to 4.0×10^6.

The application of these static properties to the calculation of the frequency-dependent dielectric function is questionable. At finite times the mean-field approximation is expected

to break down; the field experienced by the dipoles may be expected to be neither spatially uniform nor to have the same value as at infinite time. For these reasons full calculations of the frequency-dependent permittivity have not been attempted.

4. Discussion

The calculations reported here have been derived almost from first principles according to specific interpretations of the simple superparaelectric model. The uncertainties of the averaging of the cluster permittivities dictates that the results of calculations can be taken only as a guide to the behaviour resulting from the initial assumptions. Consequently, no explicit attempt has been made, other than qualitative comparison, to fit the results to experimental data from relaxors. It is clear, however, that in choosing the various conditions for the simulations, some guidance has been taken from the literature.

Given that quantitative comparison with experimental data has yet to be carried out, the assumption that the clusters may be treated as individual classical ferroelectrics is shown to be a useful working hypothesis. Even without invoking a distribution of Curie temperatures, the finite-size constraints predict local polarization fluctuations above T_0 and, consequently, a departure from Curie–Weiss behaviour up to approximately $T_0 + 200$ K, as seen experimentally in PMN. In general, the size of the clusters for which the model predicts relaxor-like properties is similar to those inferred from TEM [8, 9], and x-ray and neutron diffraction [10, 23].

From the results of the case of independent mono-sized clusters, it becomes clear that it is possible to have a peak in the real part of permittivity as a function of temperature which is unrelated to any structural change and displays frequency dependence similar to that observed in relaxors. However, the imaginary part is in general agreement with relaxors only when a distribution of the size of polar regions is introduced. These first two cases, where the regions are independent and the size is temperature independent, correspond to a dipolar glass but without ferroelectric order. Although this is certainly a possible interpretation of relaxor behaviour, the width of the permittivity peaks in the temperature domain suggest that this description is inappropriate for PMN, but is worthy of further consideration for materials such as PBZT.

The case in which the size of the regions diverge at a non-zero temperature and that in which the clusters would exhibit dipolar interactions might be considered as two aspects of the same situation. Both result in a divergence of the static permittivity at non-zero temperature, suggestive of the more narrow relaxation peaks of PMN and PST. For temperature-dependent cluster sizes, no assumptions are made concerning the mechanism of cluster coarsening, therefore the onset of longer-range ferroelectric ordering is not explicit in the calculation, however there is an implication that at some finite temperature long-range order would result. If the coarsening mechanism were a thermally activated process, the process may effectively be brought to a halt before long-range order sets in, commensurate with the slowing down of the superparaelectric moments. This picture is consistent with the measurements of the temperature dependence of relaxation time [18] and polar fluctuation correlation length [27]. On the other hand, the kinetics may favour the transition to a macro-domain state at temperatures above the divergence of the dipole relaxation time. This situation would correspond to that of PST and PSN, with a spontaneous transition from relaxor to ferroelectric.

The same arguments may be used in the example of dipolar coupling. In this case the mechanism of long-range ordering is more explicit, therefore it is possible to define a

temperature below which a macroscopic ferroelectric state is stable. Depending upon the strength of the coupling this transition may occur at temperatures when the dipole relaxation frequency is in the observable range (cf. PST and PSN) or when the frequency is well below our normal experimental range. The latter corresponds to the case of the ferroelectric dipolar glass cited by Yushin [14] for PMN.

More insight into the relationship between cluster growth and dipolar coupling might be obtained from Monte-Carlo-type simulations in which the two phenomena would be independent of the form of cluster interactions chosen. However, given some of the qualitative successes of the present naïve approach, it would be instructive to attempt fitting some elements of the model to experimental data. As already shown by Viehland [2] a Curie constant and T_0 can be extracted from high-temperature dielectric data. In addition, analysis of polarization field data according to equation (3) can yield values for $P_s(T)$ and $\bar{\lambda}(T)$. This would, on the one hand, determine how close to reality is the assumption of ferroelectric-like clusters, and on the other, confirm the form of the temperature dependence of cluster size and its role in determining T_f.

5. Conclusions

A method of calculating the dielectric behaviour resulting from the superparaelectric model of relaxors has been proposed. For a fictitious superparaelectric based on $Pb(Zr_{0.7}Ti_{0.3})O_3$, it is shown that departures from normal ferroelectric behaviour becomes significant when the size of coherently polarizing regions is less than 15 nm. The predictions of a depression of the permittivity around T_0 and of high-temperature polarization fluctuations are consistent with experimental observations. The results from a limited number of scenarios suggests that a model involving a distribution of sizes and some coupling of the superparaelectric regions, expressed here as either dipolar interactions or rapid coarsening with decreasing temperature, provides the best qualitative fit to relaxor behaviour. This picture is consistent with the interpretation of a relaxor as a dipolar glass with ferroelectric ordering.

Acknowledgments

The author wishes to thank: F Chu and A Glazounov of the Ceramics Laboratory, EPFL for the data in figure 1, Professor L E Cross for useful discussions concerning the superparaelectric/dipolar glass model and the Fonds National Suisse de la Recherche Scientifique for financial support of the relaxor programme in the Ceramics Laboratory, EPFL.

References

[1] Cross L E 1987 *Ferroelectrics* **76** 241
[2] Viehland D, Jang S J, Cross L E and Wuttig M 1992 *Phys. Rev.* B **46** 8003
[3] Burns G and Dacol F 1983 *Solid State Commun.* **48** 853
[4] Viehland D, Li J F, Jang S J, Cross L E and Wuttig M 1992 *Phys. Rev.* B **46** 8013
[5] Chu F, Reaney I M and Setter N 1993 *Ferroelectrics* at press
[6] Smolenskii G A 1970 *J. Phys. Soc. Japan* **28** 26
[7] Setter N and Cross L E 1980 *J. Appl. Phys.* **51** 4356
[8] Chen J, Chan H and Harmer M 1989 *J. Am. Ceram. Soc.* **79** 593
[9] Randall C and Bhalla A 1990 *J. Mater. Sci.* **29** 5

[10] de Mathan N, Husson E, Calvarin G, Gavarri J R, Hewat A W and Morell A 1991 *J. Phys.: Condens. Matter* **3** 8159
[11] Höchli U T, Knorr K and Loidl A 1990 *Adv. Phys.* **39** 405
[12] Kirollov V and Isupov V 1973 *Ferroelectrics* **5** 3
[13] Viehland D, Jang S J, Cross L E and Wuttig M 1990 *J. Appl. Phys.* **68** 2916
[14] Yushin N K and Dorogovtsev S N 1993 *Ferroelectrics* **143** 49
[15] Westphal V, Kleeman W and Glinchuk M D 1992 *Phys. Rev. Lett.* **68** 847
[16] Viehland D, Jang S, Cross L E and Wuttig M 1991 *Phil. Mag.* B **64** 335
[17] Chu F, Setter N and Tagantsev A K 1993 *J. Appl. Phys.* at press
[18] Colla E V, Koroleva E Yu, Okuneva N M and Vakhrushev S B 1992 *J. Phys.: Condens. Matter* **4** 3671
[19] Haun M J, Furman E, Jang S J and Cross L E 1989 *Ferroelectrics* **99** 13
[20] Haun M J, Furman E, McKinstry H A and Cross L E 1989 *Ferroelectrics* **99** 27
[21] Haun M J, Zhang Z Q, Furman E, Jang S J and Cross L E 1989 *Ferroelectrics* **99** 45
[22] Haun M J, Furman E, Halemane T R and Cross L E 1989 *Ferroelectrics* **99** 55
[23] Haun M J, Furman E, Jang S J and Cross L E 1989 *Ferroelectrics* **99** 63
[24] Devonshire A F 1954 *Adv. Phys.* **3** 85
[25] Bell A J 1993 *Ferroelectrics Lett.* **15** 133
[26] Moulson A J and Herbert J M 1990 *Electroceramics* (London: Chapman and Hall) p 80
[27] Vakhrushev S B, Kvyatkovsky B E, Nabereznov A A, Okuneva N M and Toperverg B P 1990 *Ferroelectrics* **90** 173